

Codoping: A possible pathway for inducing ferromagnetism in ZnO

N. N. Lathiotakis*

Theoretical and Physical Chemistry Institute, NHRF, 48 Vassileos Constantinou, 11635 Athens, Greece

Antonios N. Andriotis†

Institute of Electronic Structure and Laser, FORTH, P.O. Box 1527, 71110 Heraklio, Crete, Greece

Madhu Menon‡

*Department of Physics and Astronomy, University of Kentucky, Lexington, Kentucky 40506-0055, USA
and Center for Computational Sciences, University of Kentucky, Lexington, Kentucky 40506-0045, USA*

(Received 8 April 2008; revised manuscript received 10 October 2008; published 24 November 2008)

A detailed *ab initio* (DFT/GGA and DFT/GGA+*U*) investigation of codoping ZnO with Co and Cu ions reveals the role of Cu and the existence of optimum structural dopant configurations which could lead to the enhancement of ferromagnetism. The role of the Cu ions in Zn(Co,Cu)O is to act as superexchange mediators while causing a remote delocalization through the hybridization of the Cu $d_{3z^2-r^2}$ spin-majority states with the O *p* states, thereby enhancing the ferromagnetism. The ferromagnetic state is found to be more favorable than the antiferromagnetic one if the Cu-*d* band is *spin splitted*. Such a process is reminiscent of the conventional RKKY interaction among magnetic impurities embedded in a metal.

DOI: [10.1103/PhysRevB.78.193311](https://doi.org/10.1103/PhysRevB.78.193311)

PACS number(s): 71.20.-b, 73.20.Hb, 75.30.Et, 75.30.Hx

The role of defects in developing ferromagnetism (FM) is well known. In particular, the study of doped ZnO has attracted much attention lately. Electron paramagnetic resonance (EPR) measurements has led to the conclusion that the observed magnetic signal from *n*-type samples of Co⁺⁺-doped ZnO [to be denoted as Zn(Co)O] should be attributed to states other than the $3d^7$ Co states,¹ while magnetic circular dichroism (MCD) has shown that room-temperature ferromagnetism in Zn(Co)O could be attributed to the hybridization of the conduction band of the doped ZnO with some of the *d* electrons of the magnetic ions.² Magnetism was also observed in ZnO doped with most of the other $3d$ elements, among which the magnetism of the low-doped Zn(Mn)O leads to the conclusion that it can be induced by either localized defect states or band states.²

From the viewpoint of theory, the outcome for the relative stability of the ferromagnetic (FM) and antiferromagnetic (AFM) states of the Co-doped ZnO depends on how accurately the *e-e* correlations are treated by the computational method used.³ Thus, some of these *nm* Co configurations were found to exhibit FM and some others AFM ground state according to the density-functional theory (DFT) results within the local-density approximation (LDA). However, in the LDA+*U* approximation all the *nm* Co configurations studied were found to prefer the AFM ordering.^{3,4}

On the other hand, the ferromagnetic exchange interaction found between Cu ions, in the Cu-doped ZnO, is attributed to the hole states delocalized via a *p-d* hybridization,⁵ leading to the conclusion that the existence of holes and metallicity are the necessary conditions to obtain high ferromagnetic stability.⁵ This conclusion is at odds with the findings of Ye *et al.*,⁶ who demonstrated that the ferromagnetism in Cu-doped ZnO is not related to the hole density but rather to the inherent properties of the CuO₄ tetrahedra and the associated hybridization among them.

In our recent reports, we pointed out the common origin of magnetism in the nontraditional inorganic materials [as,

for example, that of some diluted magnetic semiconductors (DMSs), e.g., Zn(Co)O] and that of the C₆₀-based polymers.⁷⁻¹⁰ More specifically, the magnetism of these materials was attributed to the *simultaneous presence* of two kinds of defects (of structural/topological or of substitutional-impurity type) forming chains of alternating effective *donor* (*D*) and *acceptor* (*A*) crystal sites,¹¹ which could induce *selective remote delocalization*, leading to significant charge- and spin-density transfers which take the form of charge-density-like waves (CDWs) and spin-density-like waves (SDWs).¹²

Recently, *codoping*, i.e., the *simultaneous presence* of two kinds of defects, has attracted attention primarily because of the possibility of using it to tailor the position and occupancy of the Fermi energy (E_F) of the doped DMS.¹³⁻¹⁹ Thus, codoping with shallow acceptors and donors was viewed as a potential means to specify the availability of carriers to mediate ferromagnetism.¹³⁻¹⁸

In the present work, we report results of a detailed investigation of the codoped Zn(Co,Cu)O DMS and demonstrate the key role of the Cu⁺ codopants in developing the magnetic features of the Zn(Co,Cu)O system. We performed a DFT plane-wave calculation²⁰ with ultrasoft pseudopotentials using the generalized gradient approximation (GGA) functional and the GGA+*U* approximation. The supercell consisted of hexagonal $3 \times 3 \times 3$ cell containing 108 atoms. The supercell size is large enough to allow us to investigate a large number of different dopant and codopant geometric structures and isolate the interaction between impurities (dopant concentrations 4%–5%). Due to the big size of the supercell, we considered only two *k* points, for which we chose the *k* points introduced by Chadi.²¹ We verified the adequacy of this choice by increasing the number of *k* points. No significant differences in the corresponding electron DOS's were found by going to a $4 \times 4 \times 4$ Monkhorst-Pack. Also, the differences in total energy between FM and AFM configurations (which is the quantity of interest) was found

to change by less than 10% if the number of k points were increased to eight. The kinetic-energy cutoff for the charge density and the potential was chosen to be 200 Ryd, and a Gaussian smearing parameter equal to 10^{-2} was used as a result of the small metallicity introduced by the doping. For all the structures, the spin-up and spin-down densities were fully converged.

In order to improve upon the deficiencies of the DFT/GGA (i.e., underestimation of the band gap and the overestimation of the Zn d O p hybridization²²), we used the LDA+ U approach. Our choice for the Hubbard U parameters is $U_{\text{Zn}}=6.5$ eV, $U_{\text{Co}}=2.5$ eV, and $U_{\text{Cu}}=1.0$ eV. With this choice, the positions of the Zn d and the Co d impurity bands are in best agreement with experiment.²³ Our values for Hubbard U correspond to the U - J differences, where U and J denote the intrasite Coulomb and exchange interactions, respectively, and compare well with other theoretical investigations.^{24–26} It should be noted, however, that the comparison among the various sets of the U parameters used by various LSDA+ U implementations is meaningful only if it refers to similar implementations. More precisely, it depends strongly on the pseudopotential choice, the normalization of the atomic wave functions, the way occupancies and site-projected terms are evaluated, as well as the computational characteristics of each computer code that is employed.²⁷ It should further be noted that the employment of the LSDA+ U level with U terms for the d states only does not improve upon the energy gap. This can be achieved by including U terms for the p electrons as well and, in particular, for the O p states. Recent investigations confirm that in this case the FM coupling prevails upon doping with carriers.²⁶

In the $3 \times 3 \times 3$ ZnO superlattice structure, we first substitute two of the Zn atoms with Co atoms forming four different structures: C1, C2, D, and E. In the first two (C1 and C2), the two Co impurities are first neighbors. In the first (C1), they lie on the same Zn plane perpendicular to the hexagonal c axis, while in the second they lie on two adjacent planes. In the third and fourth (D and E), the Co atoms lie in second- and third-nearest-neighbor Zn planes, respectively. These structures were further doped with a Cu atom in various positions. All these structures with a codopant Cu atom are shown in Fig. 1. The numbering following the Cu atoms in the figure denotes the number of the Zn atom substituted by Cu in our supercell.

Our detailed analysis has shown that the Co $3d$, the O $2p$, and the Cu $3d$ projected bands all span the same energy space, just below the Fermi energy for the majority spin and cross the Fermi energy for the minority spin (see Fig. 2). Thus, the interaction of the Co magnetic d states involves their hybridization with the O $2p$ and Cu $3d$ states, while both O and Cu atoms acquire significant net magnetic moments (see below). In addition to these observations, some important additional trends can also be obtained from our results. In particular: (i) The FM enhancement is found in structural configurations in which the two Co atoms are located in different Zn planes in the Zn sublattice within the range of third nm . (ii) The Cu-induced FM enhancement is more pronounced when the Cu atoms are located between the Co atoms (e.g., D-Cu55, D-Cu41) or in a highly symmet-

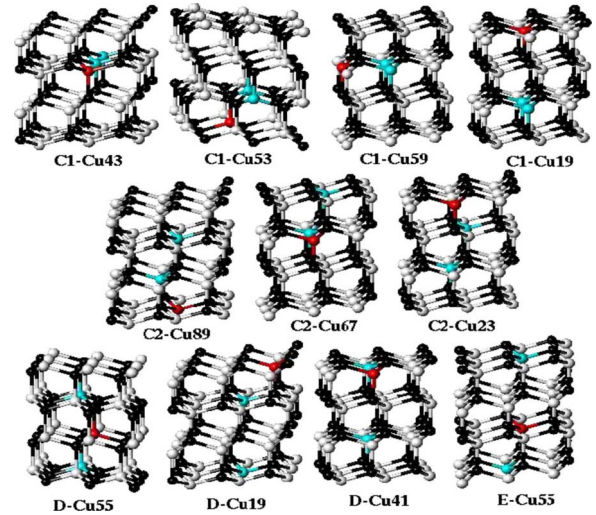


FIG. 1. (Color online) The structures of ZnO with the impurity Co atoms (blue/light gray) and the Cu impurities (red/dark gray).

ric position in the proximity of Co (e.g., C1-Cu53). (iii) Comparing the FM and the AFM states of a particular structure, it is observed that the structure for which the FM state is more stable corresponds to an AFM state in which the magnetic moment on the Cu atom is zero (e.g., D-Cu55). The FM and AFM states become degenerate if the splitting of the Cu d band is the same for both FM and AFM states (e.g., D-Cu19). Thus, *the FM state becomes more favorable because the Cu d band is spin splitted*. When the AFM state also supports such a splitting, then it is either favorable (like C1-Cu59) or the FM and AFM states are almost degenerate (like D-Cu19) (see Fig. 2). (iv) Magnetic enhancement

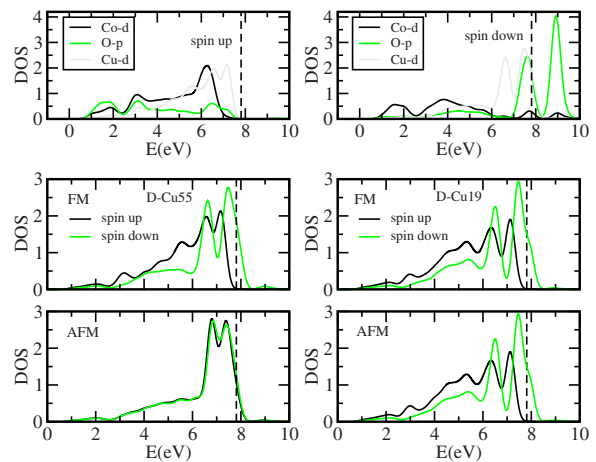


FIG. 2. (Color online) Top panel: The Co- d -, O- p -, and Cu- d -projected DOS for the D-Cu55 structure (of Fig. 1). The Fermi energy is indicated by the vertical dashed line. The position of the bands in the energy scale supports a strong hybridization of these bands. The oxygen atom chosen for the projection is the one neighboring both the Co and Cu atoms. Bottom (double) panel: The Cu- d -projected DOS for D-Cu55 (left) compared to D-Cu19 (right) for the FM and AFM states demonstrating the lack of splitting of the former in contradistinction to the splitting of the latter for the AFM states. The lack of splitting in the AFM configuration leads to strong FM behavior.

TABLE I. Results for the structures shown in Fig. 1 obtained using the DFT/GGA for the total-energy difference between the AFM and FM configurations, the total and absolute magnetization (in Bohr magnetons), and the Cu *d*-states projected magnetization for: (i) two substitutional Co impurities in ZnO and (ii) ZnO codoped with Co and Cu. All magnetizations are in Bohr magnetons. Corresponding results derived using the DFT/GGA+*U* level of approximation are shown in parentheses.

Structure	ΔE (FM-AFM) (meV)	Magnetization		Absolute magnetization		Cu magnetization	
		FM	AFM	FM	AFM	FM	AFM
Only two Co impurities:							
C1	42.50	6.0	0.0	6.11	5.87		
(C1)	(45.34)	(6.0)	(0.00)	(6.10)	(5.90)		
C2	0.716	6.0	0.0	6.12	5.95		
(C2)	(14.64)	(6.0)	(0.00)	(6.10)	(5.90)		
D	-0.802	6.0	0.0	6.14	6.11		
(D)	(-0.400)	(6.0)	(0.00)	(6.10)	(6.10)		
E	-0.026	6.0	0.0	6.14	6.13		
With Cu co-doping:							
D-Cu55	-65.9	7.08	0.05	7.25	6.90	0.47	0.03
(D-Cu55)	(-44.2)	(7.00)	(0.05)	(7.14)	(6.76)	(0.47)	(0.03)
D-Cu19	-1.9	7.06	0.78	7.24	7.20	0.52	0.52
(D-Cu19)	(87.5)	(7.00)	(1.00)	(7.15)	(7.13)	(0.57)	(0.65)
D-Cu41	-71.8	7.05	0.01	7.23	6.87	0.47	0.06
C1-Cu43	-4.7	7.05	0.01	7.20	6.56	0.45	0.01
C1-Cu53	-56.8	7.03	0.01	7.18	6.45	0.49	0.00
(C1-Cu53)	(-125.3)	(7.00)	(0.00)	(7.15)	(6.37)	(0.63)	(0.00)
C1-Cu59	33.9	7.03	0.74	7.18	6.91	0.50	0.49
(C1-Cu59)	(7.4)	(7.00)	(1.00)	(7.15)	(6.91)	(0.65)	(0.62)
C1-Cu19	-22.8	7.03	0.02	7.18	6.62	0.50	0.04
C2-Cu89	-2.1	7.05	0.78	7.22	7.0	0.51	0.51
(C2-Cu89)	(14.9)	(7.00)	(1.00)	(7.15)	(6.98)	(0.65)	(0.64)
C2-Cu67	-35.2	7.04	0.71	7.20	6.87	0.46	0.45
(C2-Cu67)	(8.3)	(7.00)	(1.00)	(7.14)	(6.89)	(0.62)	(0.64)
C2-Cu23	-99.2	7.02	0.03	7.19	6.29	0.49	0.00
E-Cu55	-0.8	7.07	0.75	7.25	7.23	0.51	0.51

seems to have its origin in the inter-Zn-plane interactions. The intra-Zn-plane interactions seem to be of minor effect in the development of ferromagnetism or lead to AFM states (e.g., C1-Cu43, C1-Cu59). (v) The magnetic configurations which show enhanced magnetic features are by far the most stable ones.

Our findings are summarized in Table I. In the absence of any additional impurities, and within the DFT/GGA, the AFM state seems to be more stable for the two Co atoms if they are first neighbors in the Zn sublattice. This behavior is even more pronounced by the introduction of Hubbard *U* correction (see “Only two Co impurities,” top part of Table I). This result is in agreement with other calculations.^{3,28,29} For larger interatomic distances, the FM configuration is favorable but the energy difference between the two states is very small. In the presence of an additional Cu impurity we observe (within the DFT/GGA) a significant enhancement of

the stability of the FM state versus the AFM one. The FM coupling was found more stable in all the geometries studied except one (see bottom part of Table I). On the other hand, while the stability of the FM phase is reduced relative to that of the AFM one at the LSDA+*U* level, it does not affect our conclusions indicating that the participation of the Cu codopant in the hybridization of the Co 3*d*-O 2*p* orbitals dominates the *e-e* correlations. Again, in these cases the FM arrangement is observed when Cu is not magnetized in the AFM configuration. A noticeable difference between the DFT/GGA and the DFT/GGA+*U* results is that the acquired magnetic moment on Cu is found larger in the DFT/GGA+*U* case. That is, when AFM prevails, the total magnetization is higher than for pure GGA by 0.3 Bohr magnetons.

Our results reconfirm previous findings^{12,29} that codoping Zn(Co)O with Cu results in stable FM ground-state configurations. However, the picture we obtained for the role of Cu⁺

in enhancing the FM stability between the magnetic impurities is quite different. In particular, it is found that the role of Cu^+ is analogous to that played by the free electron in the development of the Ruderman-Kittel-Kasuya-Yosida (RKKY) interaction. The Cu^+ ion, being spin polarized by the presence of the magnetic impurities (as shown in Fig. 2), “communicates” the disturbance to its neighboring magnetic impurities, thus, mediating an indirect magnetic interaction among them. Similar interpretation can also be given for the results of Ye *et al.*,⁶ as seen in their Table I, where a change in polarization of the interstitial charge can be observed when switching from the FM to the AFM state. Given the half-metallic character of the $\text{Zn}(\text{Co,Cu})\text{O}$ system (see Fig. 2, top panel), a small contribution of the conventional RKKY mechanism mediating ferromagnetism can also be expected; however, not to the extent of the spin-polarization mechanism of the mediating Cu ions due mainly to the large separations between the Co ions. It could then be said that the $\text{Zn}(\text{Co,Cu})\text{O}$ system gives us a clear demonstration of the way an RKKY-like mechanism for ferromagnetism evolves in a semiconducting system, i.e., in the absence of charge carriers, taking the form of a superexchange interaction.

In contradistinction to the free-electron case, the Cu-mediated interaction is highly anisotropic as evidenced by the strength of the calculated FM coupling for the various configurations shown in Table I. We attribute this behavior to the band filling of the d orbitals of Cu and their *directionality*. This is supported by our findings that the $\text{Cu } d_{3z^2-r^2}$ states (the z axis taken to be along the hexagonal close pack c axis) split more than the remaining d states of Cu. In the cases that ferromagnetism is pronounced, no splitting of these states is found in the AFM state. In the AFM state, the $\text{Cu } d_{3z^2-r^2}$ are almost degenerate with the other d states, especially the $d_{x^2-y^2}$ and the d_{xy} . In the FM state, on the other hand, this degeneracy is lifted, leading to a lowering of energy.

The superexchange form of the interaction of the Co at-

oms follows a path through the O and Cu atoms. The key mechanism is the hybridization of the Co d states with the O p and subsequently with the Cu d states. In the structures with pronounced ferromagnetism, the hybridization of the Cu d states with the O p is particularly enhanced. That effect is assisted by the downwards shift of the Cu $d_{3z^2-r^2}$ spin-majority band which overlaps (in energy scale) with the O p band. This mechanism was more evident for the structures D-Cu55, C1-Cu53, and C2-Cu23, which are all found to be strongly FM. Clearly, the enhancement of the hybridization results in additional delocalization of the Cu $d_{3z^2-r^2}$ bands analogous to that found in the case of C_{60} -based magnetic polymers.¹² I.e., the p - d hybridization induces a remote electron delocalization which mediates the Co-Co interaction. This observation is in partial support of the conclusion arrived at by Ye *et al.*,⁶ who attributed the magnetic features of the $\text{Zn}(\text{Cu})\text{O}$ to the inherent properties of the CuO_4 tetrahedra and their coupling.

In conclusion, it has been demonstrated that in codoped $\text{Zn}(\text{Co,Cu})\text{O}$ there exist optimum structural dopant configurations which lead to the enhancement of ferromagnetism. The role of the Cu^+ ions in $\text{Zn}(\text{Co,Cu})\text{O}$ is to act as superexchange mediators by causing a remote delocalization through the hybridization of the Cu $d_{3z^2-r^2}$ spin-majority states with the O p states, thereby enhancing the ferromagnetism. Based on our findings we propose that ZnO grown by beam epitaxy, during which the doping of Co and Cu ions takes place in successive layers along the Zn planes of the Zn sublattice, could lead to a material with enhanced magnetic properties.

The present work is supported by U.S.-ARO (Grant No. W911NF-05-1-0372), DOE (Grants No. DE-FG02-00ER45817 and No. DE-FG02-07ER46375), Deutsche Forschungsgemeinschaft (Program No. SPP 1145), and by the NANOQUANTA Network of Excellence.

*lathiot@physik.fu-berlin.de

†andriot@iesl.forth.gr

‡madhu@ccs.uky.edu

¹P. Sati *et al.*, Phys. Rev. Lett. **96**, 017203 (2006).

²J. R. Neal *et al.*, Phys. Rev. Lett. **96**, 197208 (2006).

³S. J. Hu *et al.*, Phys. Rev. B **73**, 245205 (2006).

⁴T. Chanier *et al.*, Phys. Rev. B **73**, 134418 (2006).

⁵L. M. Huang *et al.*, Phys. Rev. B **74**, 075206 (2006).

⁶L. H. Ye *et al.*, Phys. Rev. B **73**, 033203 (2006).

⁷A. N. Andriotis *et al.*, Phys. Rev. Lett. **90**, 026801 (2003).

⁸A. N. Andriotis *et al.*, *Clusters and Nano-Assemblies: Physical and Biological Systems*, edited by P. Jena and S. N. Khanna and B. K. Rao (World Scientific, Singapore, 2005).

⁹A. N. Andriotis *et al.*, J. Phys.: Condens. Matter **17**, L35 (2005).

¹⁰A. N. Andriotis *et al.*, Europhys. Lett. **72**, 658 (2005).

¹¹H. M. McConnell, Proc. Robert A. Welch Found. Conf. Chem. Res. **11**, 144 (1967).

¹²A. N. Andriotis *et al.*, Int. J. Nanotechnol. **6**, 164 (2009).

¹³M. J. Reed *et al.*, Appl. Phys. Lett. **86**, 102504 (2005).

¹⁴K. R. Kittilstved *et al.*, Phys. Rev. Lett. **94**, 147209 (2005).

¹⁵N. Ozaki *et al.*, Appl. Phys. Lett. **87**, 192116 (2005).

¹⁶M. H. Kane *et al.*, J. Cryst. Growth **287**, 591 (2006).

¹⁷N. Ozaki *et al.*, Phys. Rev. Lett. **97**, 037201 (2006).

¹⁸S. Kuroda *et al.*, Nature Mater. **6**, 440 (2007).

¹⁹T. Dietl, Nature Mater. **5**, 673 (2006).

²⁰Plane-Wave Self-Consistent-Field (PWSCF) code (<http://www.pwscf.org/>).

²¹D. J. Chadi *et al.*, Phys. Rev. B **8**, 5747 (1973).

²²S. Massidda *et al.*, Phys. Rev. B **52**, R16977 (1995).

²³B. Sanyal *et al.*, J. Appl. Phys. **103**, 07D130 (2008).

²⁴S. Z. Karazhanov *et al.*, Phys. Rev. B **75**, 155104 (2007).

²⁵S. Lany *et al.*, Phys. Rev. B **77**, 241201(R) (2008).

²⁶A. Walsh *et al.*, Phys. Rev. Lett. **100**, 256401 (2008).

²⁷Hu *et al.* (Ref. 3) used implementation identical to the present work and obtained values for U that are substantially smaller.

This discrepancy can be traced back to the normalization of the pseudopotential atomic wave functions.

²⁸E. C. Lee *et al.*, Phys. Rev. B **69**, 085205 (2004).

²⁹R. Janisch *et al.*, J. Phys.: Condens. Matter **17**, R657 (2005).